Available online at www.sciencedirect.com
SCIENCE DIRECT®
Journal of Photochemistry and Photobiology A: Chemistry 156 (2003) 171–177
Journal of Photochemistry and Photobiology A:Chemistry
www.elsevier.com/locate/jphotochem

Photocatalyst TiO_2 supported on glass fiber for indoor air purification: effect of NO on the photodegradation of CO and NO_2

C.H. Ao[a], S.C. Lee[a,*], Jimmy C. Yu[b]

[a] *Department of Civil and Structural Engineering, Research Center for Urban Environmental Technology and Management, The Hong Kong Polytechnic University, Hong Hom, Kowloon, Hong Kong, China*
[b] *Department of Chemistry and Materials Science and Technology Research Center, The Chinese University of Hong Kong, Shatin, New Territories, Hong Kong, China*

Received 15 October 2002; received in revised form 16 December 2002; accepted 16 December 2002

Abstract

A synthetic photocatalyst TiO_2 prepared using the sol–gel method showed a higher activity than commercial photocatalyst TiO_2 (P25), for the photodegradation of NO and benzene, toluene, ethylbenzene, *o*-xylene (BTEX) at typical indoor air parts-per-billion (ppb) levels. The Brunauer–Emmett–Teller (BET) surface area was found to be the vital parameter for the increased activity of the photocatalyst. The photocatalyst was immobilized on a glass fiber filter and evaluated under different humidity levels and residence time. The conversion of the synthetic photocatalyst and P25 were adversely affected by the increase of humidity, and decreased with decreasing residence time. The synthetic photocatalyst, however, was less affected by the levels of humidity. To evaluate the feasibility of photocatalytic technology for indoor air purification, other common indoor air pollutants such as CO and NO_2 at ppb levels were co-injected with NO. Results showed that the conversion of CO was not promoted by the photodegradation of NO. No competitive effect was observed between CO and NO. The presence of NO promoted the conversion of NO_2 while the conversion of NO is decreased due the competition of adsorption site on catalyst between NO and NO_2.

Keywords: Photodegradation; BET surface area; BTEX; Carbon monoxide

1. Introduction

Studies have shown that people generally spend more than 80% of time in an indoor environment [1], where pollutants such as carbon monoxide (CO), nitrogen oxides (NO_x) and volatile organic compounds (VOCs) are common and cause adverse health effects [2]. Traditional remediation techniques such as adsorption and filtration are not suitable and cost-effective for such low concentration pollutants [3]. These filters, without adequate replacement, could even become a source of VOCs in ventilation system [4]. A new approach is therefore necessary to reduce the pollutant level to maintain a clean environment for good human health.

Photodegradation using semi-conductors has proved to be a promising technology for pollution remediation [5–15]. Catalysts developed by the sol–gel method [16,17] and the addition of rare earth oxides [18,19] have received much attention. The effect of coating substrates [20,21] and the system parameters such as temperature, UV intensity, relative humidity and residence time have been investigated [22,23], but in all previous studies the concentrations evaluated were in the parts-per-million (ppm) range. The effect of photodegradation on the ppb level of indoor air pollutants is seldom reported. To our knowledge, there is no report on the synthetic photocatalyst for indoor air purification and the concurrent photodegradation of CO with NO at ppb level.

NO_x is chosen because it is one of the major indoor air pollutants and has deleterious health effects. The level of NO and NO_2 in indoor environments is in a range of several hundred ppb and less than a hundred ppb, respectively [24]. Studies [6,8,10] showed that the crystal size and the Brunauer–Emmett–Teller (BET) surface area have a direct impact on the photoactivity of the catalyst, but no study has identified which parameter is more important for the photodegradation of indoor air pollutant at ppb level. The aim of this study is to evaluate the synthetic photocatalyst for the photodegradation of gaseous pollutants in a typical indoor environment under different levels of humidity and residence time with reference to the commercial TiO_2 (P25). The effect of the crystal size and BET surface area is evaluated to

* Corresponding author. Tel.: +852-27666011; fax: +852-23346389.
E-mail address: ceslee@polyu.edu.hk (S.C. Lee).

1010-6030/03/$ – see front matter © 2003 Elsevier Science B.V. All rights reserved.
doi:10.1016/S1010-6030(03)00009-1

identify which parameter is more important for photodegradation of low level (ppb) pollutants. As reported previously, VOCs competed with NO for active sites on photocatalyst and NO promoted the photodegradation of VOCs [25]. An investigation of the promotion effect of NO on other common indoor air pollutants is thus of interest. CO and NO_2 are co-injected to evaluate the promotion and inhibition effect on NO as CO and NO_2 usually co-exist with NO in a typical indoor environment.

2. Experimental

2.1. Catalyst preparation

The catalyst used in this experiment was Degussa P25. The catalyst was used as received, without any pretreatment. The catalyst was imposed on a glass fiber filter (Whatman) by dipping it into a TiO_2 water suspension for 10 min and then calcinated at 120 °C for 1 h with a temperature gradient of 5.5 °C/min.

The preparation of the synthetic photocatalyst (denoted as T1) is as follows: a metal alkoxide solution of titanium isopropoxide (TTIP, Acros) was used as the starting materials. 10 g of TTIP was slowly added at room temperature to a solution of absolute ethanol (EtOH) in a breaker under vigorously stirred for 0.5 h to prevent a local concentration of the TTIP solution. EtOH mixed with nitric acid was added to the solution to promote hydrolysis. Polyethylene glycol (PEG, Acros) 600 was added to the solution and stirred for 1 h. The solution was then ultra sounded for 0.5 h and left for 24 h before being used. The molar ratio of TTIP:EtOH:PEG was 1:15:10, corresponding to 5 wt.% of TiO_2 in order to compare the photodegradation using P25 [26,27]. Photocatalyst T1 was immobilized on glass fiber by dip-coating. The glass fiber was loaded into the solution for 30 min and retracted at a rate of 10 mm/s. The glass fiber was dried at 100 °C for 2 h and then calcinated at 450 °C for 2 h at a heating rate of 5.5 °C/min in air.

2.2. Catalyst characterization

A Philips E'xpert X-ray diffractometer employing Cu Kα was used to identify the X-ray diffraction (XRD) pattern and the phase presented. An accelerating voltage of 35 kV and a current of 20 mA with a scan rate of 0.05° 2θ/s were used. The crystallite size was calculated by applying the Scherrer formula. Differential scanning calorimetry (DSC) and thermal gravity (TG) analysis was preformed using a NETZSCH instrument. A 10 mg sample was used and the heating rate was 10 °C/min in flowing air. The Brunauer–Emmett–Teller (BET) surface area was determined by nitrogen adsorption–desorption isotherm measurements at 77 K on a Micromeritics ASAP 2000 nitrogen adsorption apparatus. The samples were degassed at 180 °C before measurement.

2.3. Reactor and experimental

The detailed experimental setup has been reported elsewhere [25]. A reactor with a volume of 57 l (40.5H × 50.5L × 28W cm) with its surface coated by a Teflon film (BYTAC Type AF-21) was used for this study. Illumination was provided by a 6W UV lamp (Cole-Parmler) which emits a primary wavelength at 365 nm and its intensity was determined by a UV meter (Spectroline DRC-100X). The UV lamp was horizontally placed at the upper part of the reactor, 14 cm from both ends. UV intensity measured in all experiments was 600 μW/cm^2. The TiO_2 coated filter was supported by a Teflon film and fixed horizontally with a vertical distance of 10 cm between the UV lamp. Stainless steel sampling ports and Teflon tubing were used to connect the reactor and the analytical instruments.

A zero air generator (Thermo Environmental Inc. Model 111) was used to supply the air stream. Desired humidity of the flow was controlled by passing the zero air stream through a humidification chamber. The reactant stream and the zero air stream were connected to a mass flow calibrator (Advanced Pollution Instrumentation Inc. Model 700). The gas streams were mixed by a gas blender and the desired flow was controlled by a mass flow controller inside the calibrator. After the inlet and the outlet concentration achieved equilibrium (1 h), the UV lamp was turned on and initiated the reaction. The concentration of NO was continuously measured by a Chemiluminescence NO analyzer (Thermo Environmental Instruments Inc. Model 42c), which monitors NO, NO_2, and NO_x at a sampling rate of 0.7 l/min. CO was monitored by a Gas Filter Correlation CO analyzer (Thermo Environmental Instruments Inc. Model 48) at a sampling rate of 1 l/min. Pre-cleaned Summa canisters were evacuated for VOCs sampling. Constant VOCs sampling time was achieved using a mass flow controller. Samples of VOCs were collected at designated times during the experiment. After collection, the canister sample was first concentrated by a Nutech Cryogenic Concentrator (Model 3550A), and the trapped VOCs were separated and analyzed by Hewlett-Packard Gas Chromatograph (Model HP 6890) and quantified by a Mass Selective Detector (Model HP5973). After analysis, the canister was sequentially evacuated and pressurized with humidified zero air until all compounds detected were smaller than 0.2 ppb. TO-14 (Toxi-Mat-14 M Certified Standard (Matheson)) standard gas was analyzed using the GC/MS system seven times at 0.2 ppb to obtain the method detection limits [28].

3. Results and discussion

3.1. Characteristic of the photocatalyst

The X-ray diffraction pattern of T1 deposited on glass fiber was too weak for phase identification. Fig. 1 shows the XRD pattern of T1 powders with the same method prepared

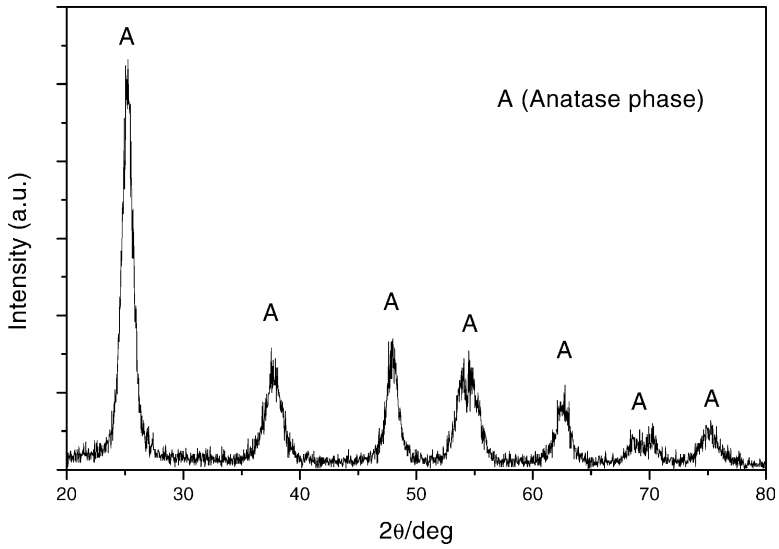

Fig. 1. XRD patterns of photocatalyst T1.

for T1 deposited on the glass fiber. The pattern was compared with the 21–1272 anatase ASTM card and 21–1276 rutile card. Only the anatase phase was found. Even when the powder was heated to 900 °C, no rutile phase and only anatase phase was found. The average crystallite size of T1 and P25 was estimated to be 9.8 and 18.8 nm using the Scherrer equation [29].

Fig. 2 shows the result of DSC–TG. Two weight loss regions were observed. From room temperature to 260 °C, a steep slope is observed and the weight loss corresponds to the desorption of absorbed water and alcohol. From 250 °C and 500 °C, a flat slope is observed and the weight loss corresponds to the residual organic and chemisorbed water. From the DSC curve, an exothermic peak was observed to be at 426 °C which corresponded to the crystallization of TiO_2 from amorphous phase to anatase phase [30]. The result also agreed with the XRD result and only the anatase phase was observed when the sample was calcinated at 450 °C.

As with of applying coated TiO_2 glass fiber for XRD detection, only powders of T1 with the same preparation was used to identify the BET surface area. The BET surface area of T1 and P25 is 96 and 46 m^2/g, respectively.

3.2. Photodegradation of NO by photocatalyst at different residence time

Fig. 3 shows the photodegradation of 200 ppb NO at a humidity level of 2100 ppmv. Each experiment set was conducted four times and the average value was reported. Results showed that the conversion of NO_x decreased with

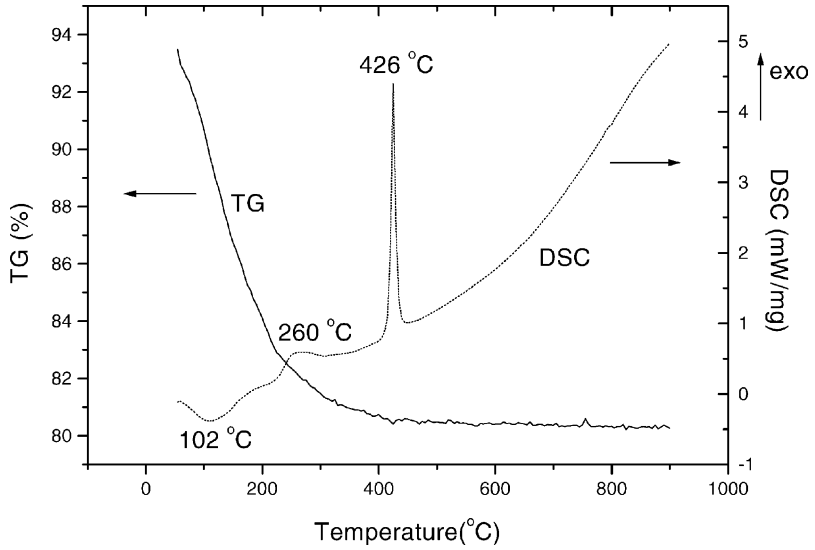

Fig. 2. DSC–TG analyses of photocatalyst T1.

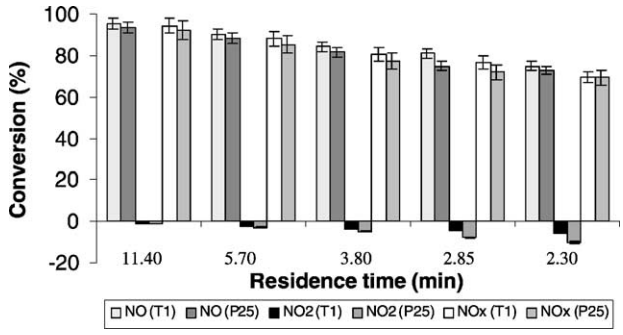

Fig. 3. Variation of NO_x at different residence time; 200 ppb NO; humidity:2100 ppmv.

decreasing residence time for photocatalyst T1 and P25. The conversion of NO_x using photocatalyst T1 and P25 decreased from 94.5 to 70.2% and 92.2 to 69.2% when the residence time decreased from 11.40 to 2.85 min. At a longer residence time, a higher rate of collision frequency between the hydroxyl radicals and the pollutants is expected and therefore the conversion of NO_x is higher [25]. The higher conversion of NO_x using photocatalyst T1 is probably due to a higher BET surface area and a smaller crystal size [6,8]. The BET surface area of T1 is nearly double that of P25. Under a low level of humidity, a higher BET surface area provides a larger adsorption site on the catalyst surface for NO to be adsorbed. Similar findings were also reported. Photocatalysts having a larger BET surface area have a higher conversion for organic compounds in the gaseous phase [26] and phenol in the aqueous phase [31].

Study [10] also showed that the photodegradation rate is also dependent on the crystal size. Maira et al. [10] showed that a smaller crystal size has a higher conversion of toluene with or without water. The result suggested that using EPR spectra, a smaller crystal size would have a more of edges and corner sites for the formation of Ti^{3+} center and form superoxide ions. It can be seen from the XRD data, photocatalyst T1 has a crystal size of 9.8 nm which is half the crystal size of P25. It is plausible that the smaller crystal size of T1 contribute the higher conversion of T1.

Table 1
Characteristics of the photocatalyst

Photocatalyst	Crystal size (nm)	Crystal phase	BET surface area (m^2/g)
T1	9.8	Anatase	96
T2	10.2	Anatase	37
P25	18.8	Anatase and rutile	46

3.3. Photodegradation of NO by photocatalyst at different levels of humidity

Fig. 4 shows the photodegradation of 200 ppb NO at a residence time of 3.8 min. Previously we reported [25] that water vapor competed with NO, at ppb levels, for the adsorption site. It is clearly shown in the figure that the NO_x conversion using photocatalyst T1 and P25 decreased with increasing humidity levels. Note that the affect on T1 is smaller than P25. It is presumed that the larger BET surface area of T1 has a larger adsorption site for the conversion of NO to NO_2, with the result that the NO_2 concentration exiting the outlet stream is smaller. As the humidity level increased, the conversion difference between T1 and P25 also increased. The increase in the BET surface area successfully improved the conversion of NO_x under the current experimental conditions. As discussed in the previous section, the smaller crystal size may also affect the conversion of NO. However, as the photocatalyst T1 has a larger BET surface area and a crystal size smaller than P25, it is difficult to distinguish at this stage whether the higher conversion of T1 is due to the smaller crystal size or the larger BET surface area. In order to evaluate the vital parameter for higher conversion, T1 was prepared without the addition of PEG 600 (denoted as T2). T2 has a similar crystal size of 10.2 nm and a BET surface area of 37 m^2/g.

3.4. Photodegradation of NO and BTEX with photocatalyst T1, T2, and P25

The effect of crystal size and BET surface area was investigated to identify the vital parameters for photodegradation of NO at ppb level. Table 1 summarizes the characteristics

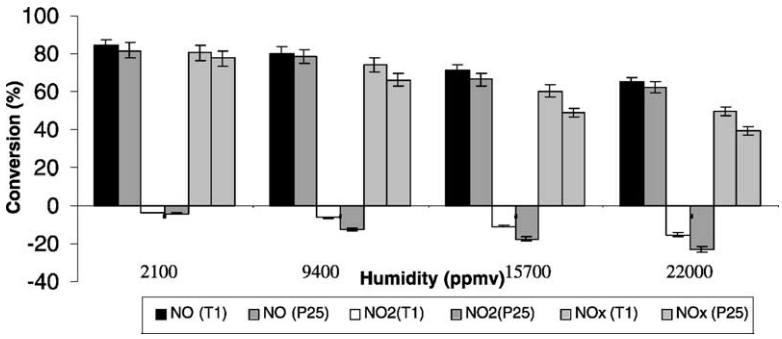

Fig. 4. Variation of NO_x at different levels of humidity; 200 ppb NO; RT: 3.8 min.

Table 2
Variation of NO_x using photocatalyst T1, T2 and P25 at different residence time

Residence time (min)	Conversion (%)								
	NO			NO_2			NO_x		
	T1	T2	P25	T1	T2	P25	T1	T2	P25
11.40	95.50	92.10	93.50	−1.02	−1.87	−1.35	94.48	90.23	92.15
5.70	90.23	87.27	88.33	−2.18	−2.63	−2.95	88.05	84.64	85.35
3.80	84.17	80.36	81.65	−3.63	−4.33	−4.87	80.54	76.03	77.45
2.85	80.88	73.58	74.75	−4.20	−8.50	−7.99	76.68	65.08	71.95
2.30	75.78	72.28	72.75	−5.61	−12.29	−10.29	70.18	59.99	69.20

200 ppb NO; humidity: 2100 ppmv.

Table 3
Variation of NO_x using photocatalyst T1, T2 and P25 at different levels of humidity

Humidity level (ppmv)	Conversion (%)								
	NO			NO_2			NO_x		
	T1	T2	P25	T1	T2	P25	T1	T2	P25
2100	84.17	73.08	81.65	−3.63	−6.22	−4.2	80.54	66.86	77.45
9400	80.23	70.94	78.65	−6.22	−17.51	−12.4	74.01	53.43	66.25
15700	71.08	62.76	66.45	−10.76	−24.13	−17.45	60.32	38.63	49.00
22000	64.98	50.99	62.25	−15.36	−28.97	−22.95	49.62	22.02	39.30

200 ppb NO; RT: 3.8 min.

of the photocatalyst conducted in this study. As shown in Table 2, the NO conversion of T2 under different residence time is lower than T1 and P25. This is probably due to the lower BET surface area of the photocatalyst T2. T2 has a BET surface area of 37 m^2/g, which is smaller than T1 and P25. The difference in NO conversion, however, is not significant, as the BET surface area of T2 is only slightly smaller than P25. The results of a comparison of photocatalysts T1 and T2, indicated that the difference between NO conversion was larger and a fact that can be attributed to larger BET surface area. Table 3 shows the conversion of NO under different levels of humidity. The conversion of NO also follows this trend, with respect to the BET surface area of the photocatalyst, in the following order: T1 > P25 > T2. Under high levels of humidity, the competition effect of water vapor indicated the significant effect of the BET surface area.

Table 4 shows the photodegradation of BTEX at an initial concentration of 35 ppb and a residence time of 3.8 min. Photocatalyst T1 has a higher conversion of benzene and toluene of 10 and 6% compared to that of P25. No significant improved activity for ethylbenzene and *o*-xylene, however, was observed at humidity 2100 ppmv. Two reasons possibly account for this. Firstly, BTEX adsorbed a different amount on TiO_2. Larson and Falconer [32] showed that *p*-xylene adsorbed on TiO_2 more than toluene, followed by benzene. The higher BET surface area of T1 provided a larger surface adsorption site, despite the effect of a combination of low level humidity plus the result of the competition between BTEX and water vapor. The conversion for benzene and toluene were thus improved. Secondly, the reaction rate of hydroxyl radicals of ethylbenzene and *o*-xylene is comparatively higher than benzene and toluene [33]. The high conversion of ethylbenzene and *o*-xylene under the current experiment conditions might hinder the improved activity of T1 [25].

The improved activity of T1 is more significant at a high level of humidity. The conversion of BTEX using photocatalyst T1 compared to P25 is even higher (Table 5). The conversion of BTEX is significantly reduced when the humidity

Table 4
Photodegradation of BTEX using photocatalyst T1, T2 and P25

Humidity (ppmv)	Photocatalyst	Conversion (%)			
		Benzene	Toluene	Ethylbenzene	*o*-Xylene
2100	T1	37.4	62.8	72.1	75.2
	T2	27.2	52.1	66.1	69.5
	P25	29.3	56.7	69.3	72.1
22000	T1	20.6	22.8	27.4	30.7
	T2	5.3	6.1	13.2	15.9
	P25	8.1	9.5	13.6	18.9

35 ppb BTEX; RT: 3.8 min.

Table 5
Photodegradation of NO co-injected with CO

Experimental conditions		Initial concentration		Conversion (%)	
Humidity (ppmv)	RT (min)	CO (ppm)	NO (ppb)	CO	NO
2100	11.4	2	0	0	0
22000	3.8	2	0	0	0
2100	11.4	2	200	0	95.50
22000	3.8	2	200	0	64.98

level was 22000 ppmv owing to the competition water vapor for active sites [25]. The extra BET surface of T1 provided more active sites for the adsorption of BTEX. It is noted that owing to the competition of water vapor for active sites, not only the conversions of benzene and toluene were improved but also those of ethylbenzene and *o*-xylene.

The effect of crystal size is not significant under the current experimental conditions. Although T2 has a smaller crystal size (10.2 nm) than that of P25 (18.8 nm), T2 has a lower NO and BTEX conversion than that of P25. The results presented in this study are contradicted with the results presented by Maira et al. [10]. This discrepancy is probably owing to the effect of water vapor and the different pollutant levels applied. These researchers conducted a toluene photodegradation at ppm levels with different crystal size photocatalyst. At ppb levels, the competition for adsorption sites between pollutants and water vapor is a thousand times when ppm levels is applied [25]. The above results suggested that the BET surface area is more vital than the crystal size of the photocatalyst for the photodegradation of ppb level pollutants at high levels humidity.

3.5. The impact of CO on the photodegradation of NO

The concentration of CO conducted in this study is 2 ppm, which is a typical indoor CO level [34]. Table 5 shows the photodegradation of NO and CO concurrently using photocatalyst T1. As shown in the table, no conversion of CO was found under different levels of humidity and residence time. This is probably due to the amount adsorbed on the TiO_2 is rather low. Vorontsov et al. [35] showed that no CO was photodegradated below 140 ppm. In this study, only an indoor CO level of 2 ppm was applied, thus, for that reason no CO conversion was observed. Previously we demonstrated the promotion effect of NO on VOCs and the competition effect of NO and VOCs under low humidity levels [25]. It is of interest to co-inject CO with NO to investigate whether there is any promotion or competition effect. As shown in Table 4, no promotion effect was observed when NO was co-injected with CO. Presumably, the amount of CO adsorbed on the photocatalyst is too small to be promoted by the hydroxyl radicals generated by the photodegradation of NO. Conversely, no competition effect of CO on NO is observed under different levels of humidity and residence time. Under typical indoor levels, no reaction and competition effect of CO was found.

3.6. The impact of NO_2 on the photodegradation of NO

It is well studied [36,37] that NO_2 is the side product from the photodegradation of NO according to the following equation [34]:

$$NO + HO_2^{\bullet} \rightarrow NO_2 + OH^{\bullet} \quad (1)$$

Surprisingly, most of the NO photodegradation studies [36–38] only applied NO at a level of ppm but the interaction between NO and NO_2 was not reported. Previously we reported the promotion of NO on VOCs [25] and it is important to study the interaction between NO and NO_2 and as they co-exist in indoor environment.

Table 6
Photodegradation of NO co-injected with NO_2

Initial concentration (ppb)		Conversion (%)	
NO	NO_2	NO	NO_2
0	45	0	59.8
0	90	0	73.8
200	0	93.6	0
200	45	90.0	77.8
200	90	85.6	85.4

RT: 11.4 min.

Table 6 shows the photodegradation of NO, NO_2, and NO co-injected with NO_2 at a residence time of 11.4 min and 2100 ppmv humidity. It clearly shows that NO promoted the photodegradation of NO_2 while the presence of NO_2 inhibited the conversion of NO. For instance, the conversion of NO_2 at 45 ppb increased from 59.8 to 77.8% under the presence of 200 ppb NO. At 90 ppb NO_2, the increased NO_2 conversion was smaller when compared to that of 45 ppb NO_2. The NO_2 conversion only increased from 73.8 to 85.4%. As the same amount of NO was used for both experiments, smaller NO_2 concentration will has a higher promotion effect as the hydroxyl radicals generated from the photodegradation of NO is higher per NO_2. The promotion effect of NO was also reported elsewhere [25]. It is also noted that the conversion of NO decreased with an increase in the amount of NO_2 co-existing in the system. The conversion of NO decreased from 93.6 to 90% and to 85.6% when 45 ppb NO_2 and 90 ppb NO_2 was co-injected, respectively. When the total amount of active sites on the photocatalyst remained the same, the total amount of pollutants per active sites decreased. The competition effect between NO and NO_2 was also reported at a concentration of 10 ppm NO [39].

4. Conclusion

The investigation of an improved photocatalyst developed by the sol–gel method immobilized on a glass fiber filter showed a higher activity than P25 for the photodegradation of NO and BTEX at typical indoor ppb levels. The BET surface area was identified to be the key factor for the photodegradation of indoor air level (ppb) pollutants. The effect of the BET surface area is more significant under high levels of humidity. No conversion of indoor levels of CO was found under the experimental conditions. When CO was co-injected with NO, no promotion effect of NO and no competition between NO and CO was observed. Promotion effect was observed on NO_2 by the hydroxyl radicals generated from the photodegradation of NO. The presence of

NO_2, however, competed with NO for active sites on catalyst and decreased the conversion of NO.

Acknowledgements

This project is funded by the Hong Kong Polytechnic University (GW-047). The authors would like to thank Mr. W.F. Tam for technical support in the laboratory. The supply of TiO_2 (Degussa P25) from Hong Kong Degussa China Ltd. is also acknowledged.

References

[1] J. Roberts, W.C. Nelson, National Human Activity Pattern Survey Data Base. United States Environmental Protection Agency (USEPA), Research Triangle Park, NC, 1995.
[2] A.P. Jones, Atmos. Environ. 33 (1999) 4535.
[3] F.I. Khan, A.K. Ghoshal, J. Loss Prev. Process Ind. 13 (2000) 527.
[4] H. Schleibinger, H. Ruden, Atmos. Environ. 33 (1999) 4571.
[5] J. Peral, X. Domenech, D.F. Ollis, J. Chem. Technol. Biotechnol. 70 (1997) 117.
[6] K. Hashimoto, K. Wasada, N. Toukai, H. Kominami, Y. Kera, J. Photochem. Photobiol. A: Chem. 136 (2000) 103.
[7] J.C. Yu, J.G. Yu, J.C. Zhao, Appl. Catal. B: Environ. 36 (2002) 31.
[8] J.L. Zhang, T. Ayusawa, M. Minagawa, K. Kinugawa, H. Yamashita, M. Matsuoka, M. Anpo, J. Catal. 198 (2001) 1.
[9] I. Nakamura, N. Negishi, S. Kutsuna, T. Ihara, S. Sugihara, K. Takeuchi, Zhao, Appl. J. Catal. A: Chem. 161 (2000) 205.
[10] A.J. Maira, K.L. Yeung, J. Soria, J.M. Coronado, C. Belver, C.Y. Lee, V. Augugliaro, Appl. Catal. B: Environ. 29 (2001) 327.
[11] O. d'Hennezel, P. Pichat, D.F. Ollis, J. Photochem. Photobiol. A: Chem. 118 (1998) 197.
[12] H. Einaga, S. Futamura, T. Ibusuki, Phys. Chem. Chem. Phys. 1 (1999) 4903.
[13] N.N. Lichtin, M. Sadeghi, J. Photochem. Photobiol. A: Chem. 113 (1998) 81.
[14] J. Blanco, P. Avila, A. Bahamonde, E. Alvarex, B. Sanchez, M. Romero, Catal. Today 29 (1996) 437.
[15] R.M. Alberici, W.F. Jardim, Appl. Catal. B: Environ. 14 (1997) 55.
[16] Y. Tanaka, M. Suganuma, J. Sol–Gel Sci. Technol. 22 (2001) 83.
[17] Y. Zhu, L. Zhang, L. Wang, Y. Fu, L. Cao, J. Mater. Chem. 11 (2001) 1864.
[18] J. Lin, J.C. Yu, J. Photochem. Photobiol. A 116 (1998) 63.
[19] A.W. Xu, Y. Gao, H.Q. Liu, J. Catal. 207 (2002) 157.
[20] J. Yu, X. Zhao, Mater. Res. Bull. 35 (2000) 1293.
[21] Y. Ma, J.B. Qiu, Y.A. Cao, Z.S. Guan, J.N. Yao, Chemosphere 44 (2001) 1087.
[22] M.L. Sauer, M.A. Hale, D.F. Ollis, J. Photochem. Photobiol. A 88 (1995) 169.
[23] Y. Luo, D.F. Ollis, J. Catal. 163 (1996) 1.
[24] C.J. Weschler, A.T. Hodgson, J.D. Wooley, Environ. Sci. Technol. 28 (1994) 2120.
[25] C.H. Ao, S.C. Lee, C.L. Mak, L.Y. Chan, Appl. Catal. B: Environ., in press.
[26] M. Mikula, V. Brezova, M. Ceppan, L. Pach, L. Karpinsky, J. Mater. Sci. Lett. 14 (1995) 615.
[27] Y.S. You, K.H. Chung, J.H. Kim, G. Sao, Korean J. Chem. Eng. 18 (2001) 924.
[28] S.C. Lee, W.M. Li, C.H. Ao, Atmos. Environ. 36 (2002) 225.
[29] M. Music, M. Gotic, M. Ivanda, S. Popovic, A. Turkovic, R. Trojko, A. Sekulic, K. Furic, Mat. Sci. Eng. B: Solid 47 (1997) 33.
[30] I.A. Montoya, T. Viveros, T. Dominguez, J.M. Canales, I. Schifter, Catal. Lett. 15 (1992) 207.
[31] X. Deng, Y. Yue, Z. Gao, Appl. Catal. B: Environ. 39 (2002) 135.
[32] S.A. Larson, J.L. Falconer, Catal. Lett. 44 (1997) 57.
[33] R. Atkinson, Atmos. Environ. 24A (1990) 1.
[34] G.G. Akland, T.D. Hartwell, T.R. Johnson, R.W. Whitmore, Environ. Sci. Technol. 19 (1985) 911.
[35] A.V. Vorontsov, E.N. Savinov, E.N. Kurkin, O.D. Torbova, V.N. Parmon, React. Kinet. Catal. Lett. 62 (1997) 83.
[36] Y. Komazaki, H. Shimizu, S. Tanaka, Atmos. Environ. 33 (1999) 4363.
[37] K. Hashimoto, K. Wasada, M. Osaki, E. Shono, K. Adachi, N. Toukai, H. Kominami, Y. Kera, Appl. Catal. B: Environ. 30 (2001) 429.
[38] T.H. Lim, S.M. Joeng, S.D. Kim, J. Gyenis, J. Photochem. Photobiol. A 134 (2000) 209.
[39] S. Matsuda, H. Hatano, A. Tsutsumi, Chem. Eng. J. 82 (2001) 183.